BIOLOGY OF REPRODUCTION **63,** 723–729 (2000)

Dynamic Changes of Cumulus-Oocyte Cell Communication During In Vitro Maturation of Porcine Oocytes[1]

Hiroyuki Suzuki,[2,3] Byeong-Seon Jeong,[4] and Xiangzhong Yang[4]

Faculty of Agriculture and Life Sciences,[3] Hirosaki University, Hirosaki 036-8561, Japan
Department of Animal Science,[4] University of Connecticut, Storrs, Connecticut 06269

ABSTRACT

Oocyte maturation is a key issue of current animal biotechnology. This study was designed to examine the morphodynamics of the cumulus-oocyte association during oocyte maturation. Porcine cumulus-oocyte complexes were recovered from slaughterhouse ovaries; matured in vitro for 0, 24, 36, and 44 h; and evaluated by scanning electron microscopy either combined or not combined with the osmium-dimethyl sulfoxide-osmium maceration (ODO) method. The cytoskeleton distribution was also observed by fluorescence staining. Prior to maturation culture (0 h), the spherical cumulus cells were tightly clustered around the oocyte, with narrow intercellular spaces. They showed active secretion at 36 h and were fully expanded at 44 h of culture. The ODO methods revealed that the cumulus cells projected numerous long and thin transzonal projections at 0 h, but these were largely disconnected at 44 h. The outer surface of the zona pellucida showed a meshwork surface regardless of time of incubation, whereas the inner surface changed from a fine fibrous surface to a spongy surface that was coated with mucin. The vitelline surface changed from a sparse distribution of short microvilli (MV) to a dense distribution of well-developed MV. Fluorescence staining showed that the cumulus cell projections consisted mainly of microfilaments, which were abundant at the germinal vesicle and metaphase-I (M-I) stages (0–24 h) but which were decreased in number at the M-II stage (36–44 h). We conclude that the cumulus-oocyte transzonal projections became disconnected between the M-I and M-II stages as a result of cumulus expansion. The cumulus-cumulus communications, however, remained intact at these stages, although the biological functions of these communications were not clear.

oocyte development, ovum

INTRODUCTION

Mammalian cumulus cells play a very important role during oocyte growth and maturation. They are known to supply nutrients [1–3] and/or messenger molecules for the development of the oocyte [4–6] and to mediate the effects of hormones on the cumulus-oocyte complex (COC) [7]. The proportion of oocytes capable of in vitro maturation (IVM) is lower when cumulus cells are previously removed [8, 9]. The maturation status of the oocyte may be directly influenced via modifications in the mode of interaction between the oocyte and the surrounding follicular cells [10]. Our previous studies in cattle [11, 12] and hamsters [13] showed that oocyte maturation was accompanied by expansion of the cumulus masses and alterations in the ultrastructure of the oocyte surface. These observations suggest that an intimate relationship exists between the surface characteristics and the maturation status of oocytes in these species. The ultrastructural morphology of porcine oocytes and the surrounding cumulus cells [14] has not been fully investigated during oocyte maturation in vitro or in vivo.

Recent studies in cattle have demonstrated that redistribution of cytoskeletal proteins coincided with cumulus expansion during oocyte maturation in vitro [15, 16]. However, the morphological changes in the cellular associations between the oocyte and its investments during oocyte maturation in the pig are poorly understood. Information relating to this would improve our understanding of oocyte maturation and provide a theoretical basis for optimizing protocols for in vitro production of embryos in pigs. Thus, the objectives of this work were 1) to evaluate the surface ultrastructural morphology of the cumulus cells, zona pellucida (ZP), and vitelline membrane of porcine oocytes and 2) to examine ultrastructural changes of the cell association between the oocyte and cumulus cells during maturation culture of porcine oocytes. Scanning electron microscopy (SEM) analysis was used throughout the study. Furthermore, fluorescence staining was employed to examine the cytoskeleton distribution, and freeze-fractured surface SEM analysis [17] was used to examine ultrastructural changes in the cumulus cell projections and the ZP inner surface during maturation.

MATERIALS AND METHODS

Preparation and Culture of Oocytes

Ovaries were collected from prepubertal gilts at a local slaughterhouse and transported to the laboratory within 1–1.5 h in Dulbecco's PBS (Gibco, Grand Island, NY) containing 0.1% polyvinyl alcohol (Sigma Chemical Co., St. Louis, MO) (DPBS-PVA) at 37°C. Porcine COCs were aspirated from antral follicles (2–5 mm in diameter) with an 18-gauge needle fixed to a 10-ml disposable syringe. Groups of 10–15 COCs were washed and transferred to NCSU23 medium supplemented with 10% (v/v) porcine follicular fluid, 10 IU/ml eCG, and 10 IU/ml hCG [18]. The COCs were cultured for 24 h, then incubated in NCSU23 without hormonal supplements until the 44-h time point in an atmosphere of 5% CO_2 at 39°C. At 0, 24, 36, and 44 h IVM, oocytes were processed for SEM and fluorescence staining.

SEM Observations for Cumulus, ZP, and Vitellus

The methods for preparing samples for SEM observations were reported previously [11, 12]. Briefly, cumulus

[1]Supported by a grant-in-aid for Scientific Research C (10660263) from the Japanese Ministry of Education, Science, Sports and Culture and the Ito Foundation (Japan). This manuscript is a scientific contribution 1931 of the Storrs Agricultural Experiment Station at the University of Connecticut.
[2]Correspondence. FAX: 81 172 39 3750;
e-mail: suzuki@cc.hirosaki-u.ac.jp

Received: 24 January 2000.
First decision: 29 February 2000.
Accepted: 11 April 2000.

ISSN: 0006-3363. http://www.biolreprod.org

TABLE 1. Meiotic progression during in vitro maturation of porcine oocytes.

Hours of maturation	Number of oocytes	Number (%) of oocytes at each maturational stage*				
		GV	ProM	MI	AI-TI	MII
0	208	183 (88.0)	21 (10.1)	4 (1.9)		
24	105	4 (3.8)	25 (23.8)	63 (60.0)	12 (11.4)	1 (1.0) A
30	181		1 (0.5)	76 (40.4)	86 (22.9)	18 (9.6) B
36	126	1 (0.8)	6 (4.8)	11 (8.7)	21 (16.7)	87 (69.0) C
44	287	2 (0.7)	1 (0.3)	3 (1.0)	29 (10.1)	252 (87.8) D

* GV, Germinal vesicle; ProM, prometaphase; MI, metaphase-I; AI-TI, anaphase-I to telophase-I; MII, metaphase-II. Values with different letters are significantly different ($P < 0.01$).

cells were removed by pipetting in calcium-free DPBS-PVA containing 0.2% hyaluronidase (H-3506, Sigma). Oocytes were then exposed to acidified DPBS-PVA (pH 2.5) for 1 min and to 0.5% pronase (P-5147, Sigma) for 3–5 min to remove the ZP. The oocytes, with or without their investments, were fixed in 3% glutaraldehyde and 0.5% paraformaldehyde in Hanks balanced salt solution (Gibco) with 0.1% polyvinyl alcohol (HBSS) for 1 h. They were washed and attached to small glass coverslips (6 × 6 mm) coated with 0.1% poly-L-lysine solution (Sigma). The samples on the coverslips were postfixed in 1% osmium tetroxide (OsO_4) in HBSS for 1 h. The fixed specimens were conductivity stained with 2% tannic acid and 1% OsO_4 solution and then dehydrated in a series of increasing concentrations of ethanol, critical-point dried, and sputter-coated with gold. Observations were made with a JSM5300 SEM (JEOL, Tokyo, Japan) at an accelerating voltage at 20 kV.

SEM Observations Following Freeze Fracture and ODO Method

The postfixed COCs were immersed in 15%, 30%, and 50% aqueous solutions of dimethyl sulfoxide (DMSO) for 30 min each in order to prevent ice-crystal damage during freezing [17]. Groups of 20 COCs were embedded in either 7% gelatin [19] or 1% chitosan plus 2.5% gelatin [20] before freezing. Specimens were frozen on a metal plate chilled with LN_2 (Eiko Engineering, Tokyo, Japan), cracked into two parts with a razor blade and hammer, and immediately placed in a 50% DMSO solution. After rinsing, samples were immersed in 0.1% OsO_4 in HBSS at 20°C [17] for 4–6 days and then fixed again in 1% OsO_4 in HBSS for 1 h. They were conductivity stained, dehydrated, critical-point dried, sputter-coated, and observed by SEM, as described above.

Fluorescent Observations

Methods for preparing samples for fluorescent observations have been reported previously [21]. Oocytes with or without cumulus cells were fixed in a microtubule stabilization buffer [15] at 37°C for 1 h, washed extensively, and blocked overnight at 4°C in the wash medium (calcium-free DPBS containing 2% BSA, 2% goat serum, 0.2% milk powder, 0.2% sodium azide, and 0.1% Triton-X). Afterwards, the fixed samples were exposed overnight (at 4°C) to anti-β tubulin primary antibodies (1:200; T-5293, Sigma), washed, and then incubated with fluorescein isothiocyanate (FITC)-conjugated secondary antibody (1:200; F-0257, Sigma) at 37°C for 2 h. After rinsing, the samples were stained with rhodamine-phalloidin (1:1000; Molecular Probes, R-415, Eugene, OR) for microfilaments for 1 h, washed again, then stained for DNA with Hoechst 33342 (10 μg/ml) in mounting medium containing PBS and glycerol (1:1); finally, samples were mounted onto slides.

The samples were viewed on an Olympus microscope (BX-FLA; Olympus, Tokyo, Japan). A U-MNIBA filter set (Olympus) was used for FITC, a U-MWIG set (Olympus) for rhodamine, and a U-MWU set (Olympus) for Hoechst. A cooled CCD video system (ImagePoint, Photometrics Ltd., Tucson, AZ) was used to obtain images on a computer, and color adjustment was performed by IPLab-Spectrum P software (Signal Analytics Corporation, Vienna, VA).

Data Analysis

Proportional data were analyzed by chi-square test.

RESULTS

Numbers of Oocytes Examined

A total of 1917 oocytes were used for either individual SEM examination (n = 1010) or fluorescence staining (n = 907). The number of oocytes observed by SEM on the fracture plane after application of the ODO method was 81 (out of 420) COCs embedded at 0 h and 26 (out of 330) COCs embedded at 44 h. The cytological analysis of oocytes at various times of maturation culture is summarized in Table 1. Eighty-eight percent of oocytes were in germinal vesicle stage at 0 h; 71% and 90% of oocytes were in metaphase-I to telophase-I at 24 h and 30 h, respectively; and 69% and 88% of oocytes were in metaphase-II at 36 h and 44 h, respectively.

Surface Ultrastructure of Cumulus-Cumulus and Cumulus-Oocyte Communications

At 0 h IVM, COCs (n = 23) displayed a compacted arrangement of spherical cumulus cells (Fig. 1a). The cumulus cells were covered sparsely with short microvilli. At 24 h IVM (n = 21), cumulus cells became oblong in shape and were intermingled with thread-like cytoplasmic projections (referred to here as intercumulus projections), and the intercellular spaces increased profoundly (Fig. 1b). At 36 h IVM, cumulus masses (n = 20) became further expanded and were covered with abundant extracellular matrix and appeared mucified (Fig. 1c). At 44 h IVM, the cumulus investments (n = 20) were even more mucified than at 36 h IVM, with practically all cells completely coated with the extracellular matrix (Fig. 1d). Furthermore, the architecture of the intercumulus projections became very fragile, and it was difficult to keep the COCs intact during preparation for SEM. As a result, the superficial cumulus cells were easily detached, and the inner layer of the cumulus mass was observed (not shown).

By using the ODO method, the ZP was either partially or completely dissolved, depending on length of maceration

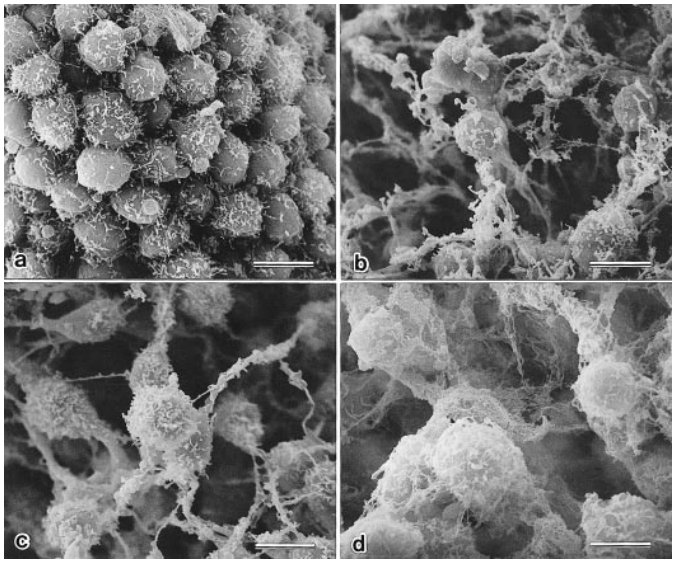

FIG. 1. Surface characteristics of porcine COCs during IVM. Bar represents 10 μm in **a–d.** **a**) 0 h IVM: spherical cumulus cells are compactly arranged where MV are frequently observed on the surface. **b**) 24 h IVM: notice the oblong-shaped cumulus cells and the increased intercellular space. An extensive network of cytoplasmic projections can also be seen among cumulus cells. **c**) 36 h IVM: notice extracellular matrix covering on the cumulus cells and elongated cellular projections among the cumulus. **d**) 44 h IVM: notice inner cumulus cells are completely covered with abundant extracellular matrix, showing mucification inside of cumulus mass.

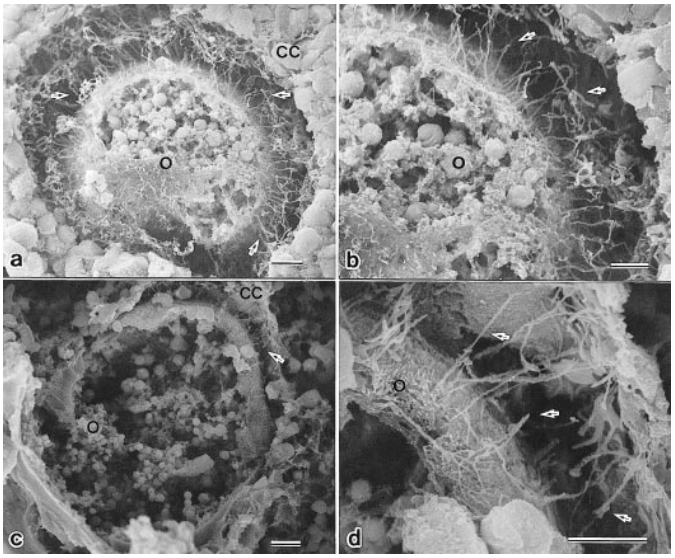

FIG. 2. Scanning electron micrographs of the porcine COC fractured and macerated. Bar represents 10 μm in **a** and **c** and 1 μm in **b** and **d.** CC, Cumulus cells; O, oocyte. Cumulus cell projections (arrows) can be seen as a result of maceration of the ZP. **a**) Fractured surface of an immature COC; **b**) higher magnification of the immature COC. **c**) Fractured surface of a mature COC; **d**) higher magnification of the mature COC. Notice that a decrease in the cumulus cell projections is evident in the matured COC (**c** and **d**) compared with the immature COC (**a** and **b**).

treatment. Following the treatment, cumulus-oocyte transzonal projections were exposed at the freeze-fractured surface. At 0 h IVM, a large number of cumulus cell projections were observed merging from the apical surface of the inner cumulus cells and reaching the vitelline surface (Fig. 2, a and b). At 44 h IVM, the cumulus cell projections decreased significantly in number, showing little direct communication between the cumulus and the oocyte (Fig. 2, c and d).

Ultrastructure of ZP Outer and Inner Surfaces

The outer surface of the ZP of porcine oocytes (n = 23, 24, 26, and 19 for 0, 24, 36, and 44 h, respectively) was basically characterized by a meshwork structure with small holes. The meshwork structure showed no dramatic changes throughout the maturation culture (Fig. 3a). In some macerated samples, a fractured inner surface of the ZP was exposed because of detachment of the oocyte vitellus from the ZP. A network of thin filaments was observed on the ZP inner surface at 0 h IVM (Fig. 3b). In contrast, the thin filaments were practically undetectable and the surface was often partially coated by a thin layer of mucified matrix at 44 h IVM (Fig. 3c). Furthermore, the ZP of the immature oocytes was dissolved in 3–4 days during the maceration period, whereas the ZP of matured oocytes was not dissolved until 6 days. Additionally, in the 44-h IVM group, the ZP clearly exhibited a heterogeneity, because the outer ZP layer was normally dissolved first, with the inner ZP layer remaining for approximately 6 days during the maceration treatment.

Surface Ultrastructure of Vitelline Membrane

The oocyte vitelline membrane was characterized by surface microvilli (MV) and occasional cytoplasmic protrusions (CP) at various densities. The CP were domelike or tonguelike in shape. The MV/CP density was arbitrarily classified as low, medium, and high, as shown in Figure 4. At 0 h IVM, the vitelline surface of all oocytes (n = 17) was characterized by low density and unevenly distributed short MV (Fig. 4a). In addition, some long and slender MV were frequently noted among short MV (Fig. 4a). At 24 h IVM, the vitelline surface in 73% (16 of 22) of oocytes remained the low-density MV pattern (10 of 16) or CP pattern (6 of 16), but the remainder showed an increased density of MV distribution, classified as medium-density MV/CP pattern (Fig. 4b). At 36 h IVM, 88% (22 of 25) of oocytes were classified as medium (60%) and high (28%) MV/CP density. At 44 h IVM, the majority of oocytes (89%, 17 of 19) had a dense population of well-developed MV (high density, Fig. 4c). Interestingly, even at 36 and 44 h, 12% and 11% of the oocytes, respectively, remained as low density. A summary of MV patterns at different maturation times is shown in Table 2.

Cytoskeleton Distribution

The cytoskeletal distribution in the COC at various maturation times was examined by actin and tubulin staining. At 0 h IVM, microfilament-filled projections at high density were observed to extend from the cumulus cells across the ZP and to terminate at the vitelline surface (Fig. 5a). The transzonal cumulus cell projections were densely stained for actin but not for tubulin. The microfilaments were also abundant at the cell-cell contact areas among cumulus cells (Figs. 5b). In contrast to transzonal cumulus cell projections, the intercumulus projections were stained intensely for both actin and tubulin (Fig. 5, c and f). The density of microfilaments in the transzonal cumulus cell projections was high and unchanged until 30 h IVM (M-I stage). At 44 h IVM (M-II stage), however, very limited numbers of microfilament-rich transzonal cumulus cell projections remained in the ZP (Fig. 5d), whereas intercumulus cell pro-

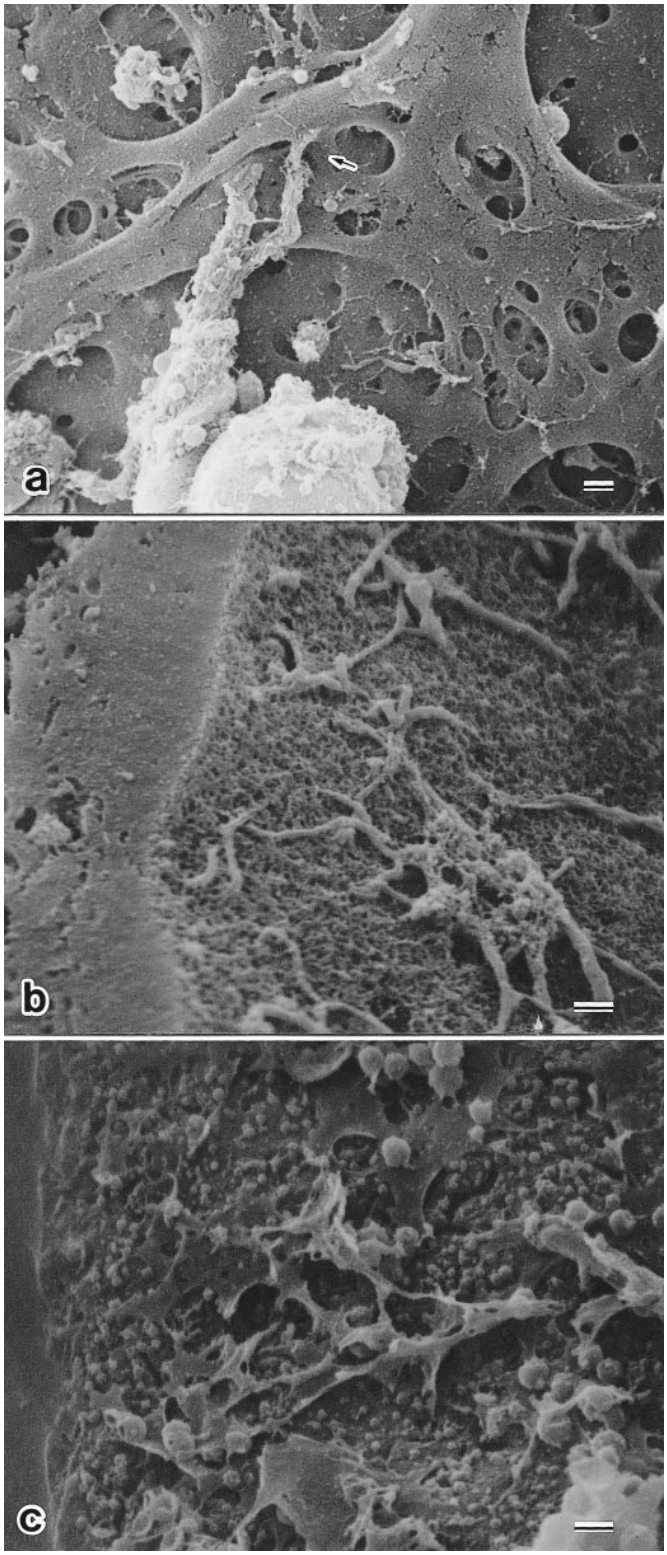

FIG. 3. Outer and inner surfaces of ZP during IVM. Bar represents 1 μm. **a**) Typical ultrastructure of porcine ZP outer surface. The outer surface is characterized by a meshwork structure, and no remarkable changes are noted during IVM. Zona pellucida at 24 h of incubation shows a corona radiata cell connecting the ZP surface with cytoplasmic projections (arrow). **b**) Inner surface of the ZP of an immature oocyte, showing a fibrous structure. Notice some terminals of transzonal cumulus cell projections. **c**) Inner surface of the ZP of a matured oocyte, showing a sponge-like surface. Notice mucus-like substance coating the inner surface at this stage.

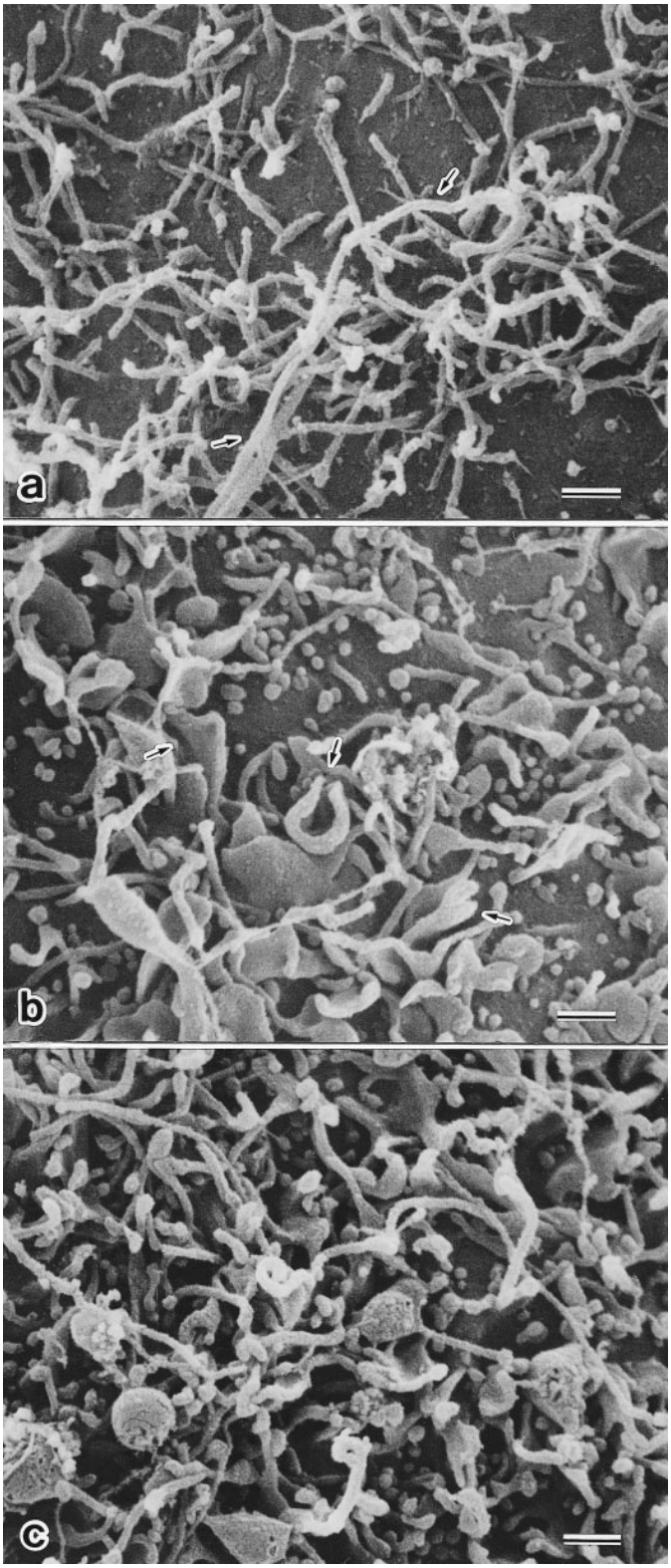

FIG. 4. Surface characteristics of vitelline membrane during IVM. Bar represents 1 μm in **a–c. a**) Low MV density pattern: an oocyte at 0 h IVM showing a sparse distribution of short MV with occasional long MV (arrows). **b**) Medium-density pattern: an oocyte at 36 h IVM displaying medium MV density. Notice a mixed distribution with tongue-shaped cytoplasmic protrusions (arrows). These protrusions are frequently observed at 24–36 h IVM. **c**) High MV density pattern: an oocyte at 44 h IVM displaying a dense distribution of MV.

TABLE 2. Oocyte surface ultrastructure at different maturation time.

Maturation time (h IVM)*	No. of oocytes	Surface microvilli density (% oocytes)			Cytoplasmic protrusions
		Low	Medium	High	
0 A	17	100	0	0	No
24 B	22	73	27	0	Yes
36 C	25	12	60	28	Yes
44 D	19	11	0	89	No

* Proportions of oocytes showing different microvilli density are significantly different in the maturation groups ($P < 0.05$ between A and B; $P < 0.01$ between others).

jections remained dense (Fig. 5e). The cumulus masses were fully expanded, with an architecture of microfilaments and microtubules (Fig. 5, e and f).

DISCUSSION

Ultrastructure of Cumulus, ZP, and Vitellus

The present SEM analysis clearly demonstrated that porcine cumulus cells manifested extensive mucification from 36 to 44 h of IVM. Fléchon et al. [14] have reported that intercellular matrix among the cumulus oophorus increased at 20 h after hCG in vivo. Therefore, there seems to be some delay in the cumulus oophorus mucification of porcine IVM oocytes compared to in vivo matured oocytes.

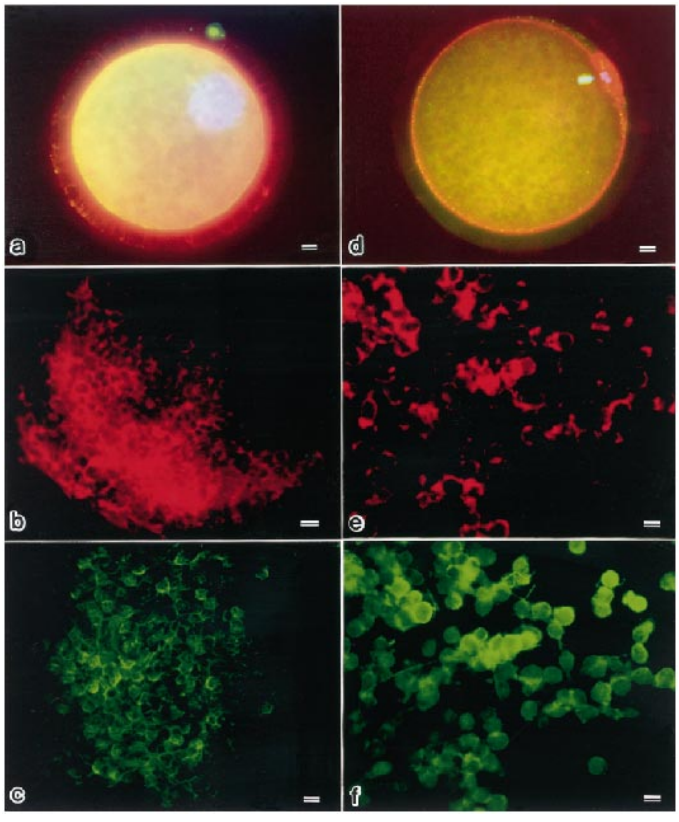

FIG. 5. Fluorescent micrographs of immature (**a–c**) and matured (**d–f**) porcine oocytes and cumulus cells. Bar represents 10 μm. Microtubules are green; microfilaments are red and nuclei/chromosomes are blue; yellow shows the overlap of microtubules and microfilaments. **a**) A GV-stage oocyte showing abundant transzonal cumulus cell projections consisting of microfilaments. **b**) Microfilament staining. **c**) Microtubule staining. Both microfilament and microtubule staining are located on the surface of the cumulus cells. **d**) An M-II-stage oocyte showing loss of transzonal cell projections. **e**) Microfilaments are located at the contact surfaces between the cumulus cells. **f**) Microtubules are seen in the cytoplasm of the cumulus cells with cytoplasmic projections between them.

Except for timing of mucification, changes in surface morphology of individual cumulus cells during the IVM observed here are very similar to those observed in those matured in vivo [14]. The surface changes in the porcine cumulus masses are similar to those reported previously in cattle [10–12, 22], mice [23–25], hamsters [13, 25], and humans [26–28]. Cumulus oophorus mucification seemed to be much greater in the pig COCs than in the bovine and hamster COCs that were examined using a similar protocol [11–13]. The reason for this difference is not clear, but it could be attributed to a species difference or to the different maturation conditions used in those studies.

As observed previously in other species, the present study documented the porous meshwork structure of porcine oocytes during maturation in vitro. The porcine ZP, however, was found to be relatively flat and less porous than the bovine ZP, which was characterized by a fibrous meshwork structure with many wide mesh holes [11, 12], but the porcine ZP resembled the ZP surface in hamsters [13, 25] and mice [25, 29, 30]. Although the outer surface of the porcine ZP did not change during IVM, the inner surface morphologies were profoundly different before versus after IVM. Similar observations had been made in the human ZP [27]. Several studies, which utilized techniques including light and electron microscopy and binding of lectins, antibodies, and a cationic dye, have revealed the apparent heterogeneity of the ZP (see review by Wassarman [31]). It has been suggested that a higher density of lectin, antibody, and ruthenium red binding sites exist in the exterior compared to the interior region of the ZP [27, 31]. Our SEM analysis demonstrated that the porcine ZP is composed of two concentric layers. Further, the degree of ZP dissolution after maceration was clearly different depending on the duration of in vitro incubation or the maturational status of the oocyte. The 44-h-incubated (or matured) ZP appeared to be considerably more insoluble (hardening) to maceration than did the 0-h-incubated (or immature) ZP. Dissolution of the incubated ZP requires more maceration time. Although the molecular basis for this difference is not clear, it is possible that some of the hardening may have been caused by the premature release of the cortical granules during the in vitro maturation culture. In cattle, it has been recently reported that the oviduct alters the ZP's digestibility by pronase, thus suggesting the role of oviductal factor(s) with regard to the block to polyspermy [32]. Further studies are needed to clarify the localization and function of the cortical granules during IVM of porcine oocytes as well as the effect(s) of oviductal factors. The observations here suggest that both morphological and physiochemical changes in the ZP may occur in the process of maturation or during in vitro incubation of the porcine oocyte.

The vitellus of immature porcine oocytes was characterized by a sparse distribution of MV. Some long and slender

MV were frequently incorporated among short MV. The long MV-like structures are likely residues or terminals of the transzonal cumulus cell projections. Such morphological characteristics were very different from those observed in cattle, in which CP were frequently noted on immature vitellus [11, 12]. In the present study, dome-like or tongue-like CP were noted only at 24–36 h IVM. During IVM, the vitelline surface of the porcine oocyte gradually changed from a sparse MV distribution pattern (low density) to a medium-density pattern and finally to a high-density MV-predominant pattern. A medium-density CP pattern was also observed during this transition. The high-density MV-predominant pattern was also noted on the matured oocytes in cattle [11, 12], hamsters [13], and mice [25, 29, 30]. Microvillous surface on the matured oocytes may be a prerequisite for sperm penetration, because the actual contribution of the MV to gamete membrane fusion has been presented [33].

Several studies showed that cell-to-cell communications via gap junctions, as well as other junctional complexes, form the major anchorage between the oocyte and cumulus cells during all stages of follicle development [3, 15, 34–39]. In the pig, the junctions between the cumulus cell projections and the oocyte are present up to 20–30 h after hCG [40]. The present observations clearly demonstrated three-dimensionally that the cumulus cell projections were directed toward and terminated at the oocyte. These transzonal projections appeared as extremely long and thin extensions and were intermingled with those arising from adjacent cumulus. These observations were in agreement with previous observations by cytochemical or transmission electron microscopic studies [15, 34–39].

The results presented here also indicated that germinal vesicle breakdown precedes the disruption of cumulus cell-oocyte projections in pigs. The cumulus cell projections remained at M-I stage in the oocytes stained by fluorescence. In addition, it was shown that a dramatic rearrangement of the cytoskeleton in the cumulus cell projections during IVM of the porcine oocytes resulted in a great reduction in microfilament-filled transzonal cumulus cell projections after maturation. Cran [40] reported changes in the distribution of organelles such as mitochondria and endoplasmic reticulum in the pig oocyte, which may parallel the redistribution of microtubules in the cytoplasm. A close association between cumulus cells and the oocyte has been shown to be important in the production of developmentally competent IVM mammalian oocytes [7, 41–43]. It is speculated that through dynamic contacts via transzonal cumulus cell projections and via intercumulus projections, some substance(s) may actively modulate the maturation of COCs. Certain factors produced by cumulus cells during follicular growth or IVM are essential for the oocyte to acquire the ability to be fertilized and to sustain normal embryo development. Cytochemical and ultrastructural observations in this study indicate that when the COC matured in vitro, the disconnection of transzonal cumulus cell projections may occur as a result of cumulus mass expansion [1] and contractions in the ooplasm [11]. After maturation, however, intercumulus projections still remained, and thus, the cumulus-cumulus cell communications were preserved. The oocyte may be firmly held by abundant extracellular matrix secreted by cumulus-corona cells, which may function in cell-cell adhesion, thereby transferring soluble factors from cumulus-corona cells to the oocytes and vice versa (see review by Salustri et al. [44]). Recent studies have pointed out the importance of glycosaminoglycans in ovarian follicles [44]. Their biological functions in ovarian biology remain to be determined. Further studies are needed to understand the significance of modifications of cumulus cell projections and the network of extracellular matrix with respect to their regulation of meiosis and acquisition of oocyte competence.

We conclude the following. Cumulus expansion and mucification profoundly occur after 24 h IVM in pigs. Coinciding with events, the transzonal cumulus cell projections are disconnected. However, why the network of intercumulus cell projections remains at the M-II stage is not clear. The ultrastructure of the oocyte membrane manifests profound changes during maturation in vitro, with low-, medium-, and high-microvilli density coinciding with immature (0-h), maturing (24–36-h), and mature (44-h) oocytes, respectively. The prolonged time of zona digestion was observed following maturation culture without any remarkable changes in the meshwork structure, although the physicochemical changes remain to be investigated in future studies.

ACKNOWLEDGMENTS

The authors thank the staff in Gene Research Center at Hirosaki University for the use of image analyzing system and the staff of the Inakadate Meat Inspection Office (Aomori, Japan). They also thank I. Fukuda and Y. Takashima for technical assistance.

REFERENCES

1. Eppig JJ. The relationship between cumulus cell-oocyte coupling, oocyte meiotic maturation, and cumulus expansion. Dev Biol 1982; 89: 268–272.
2. Haghighat N, Van Winkle LJ. Developmental change in follicular cell-enhanced amino acid uptake into mouse oocytes that depends on intact gap junctions and transport system Gly. J Exp Zool 1990; 253:71–82.
3. Laurincík J, Kroslak P, Hyttel P, Pivko J, Sirotkin AV. Bovine cumulus expansion and corona-oocyte disconnection during culture in vitro. Reprod Nutr Dev 1992; 32:151–161.
4. Lawrence TH, Beers WH, Guila NB. Transmission of hormonal stimulation by cell-to-cell communication. Nature 1978; 272:501–506.
5. Thibault C, Szollosi D, Gerard M. Mammalian oocyte maturation. Reprod Nutr Dev 1987; 27:865–896.
6. Buccione R, Schroeder AC, Eppig JJ. Interactions between somatic cells and germ cells throughout mammalian oogenesis. Biol Reprod 1990; 43:543–547.
7. Zuelke KA, Brackett BG. Luteinizing hormone enhanced in vitro maturation of bovine oocytes with and without protein supplementation. Biol Reprod 1990; 43:784–787.
8. Fukui Y, Sakuma Y. Maturation of bovine oocytes cultured in vitro: relation to ovarian activity, follicular size, and the presence or absence of cumulus cells. Biol Reprod 1980; 22:669–673.
9. Zhang L, Jiang S, Wozniak PJ, Yang X, Godke RA. Cumulus cell function during bovine oocyte maturation, fertilization, and embryo development in vitro. Mol Reprod Dev 1995; 40:338–344.
10. Familiari G, Verlengia C, Nottola SA, Tripodi A, Hyttel P, Macchiarelli G, Motta PM. Ultrastructural features of bovine cumulus-corona cells surrounding oocytes, zygotes and early embryos. Reprod Fertil Dev 1998; 10:315–326.
11. Suzuki H, Yang X, Foote RH. Surface alterations of the bovine oocyte and its investments during and after maturation and fertilization in vitro. Mol Reprod Dev 1994; 38:421–430.
12. Suzuki H, Presicce GA, Yang X. Differential surface ultrastructural characteristics and volumetric dynamics of bovine oocytes during maturation in vivo versus in vitro. J Mammal Ova Res 1998; 15:49–62.
13. Suzuki H, Fujiwara T, Yang X. Surface ultrastructural characteristics of the hamster oocyte and its investments during in vivo maturation. J Mammal Ova Res 1997; 14:191–197.
14. Fléchon JE, Motlik J, Hunter RH, Fléchon B, Pivko J, Fulka J. Cumulus-oophorus mucification during resumption of meiosis in the pig. A scanning electron microscope study. Reprod Nutr Dev 1986; 26: 989–998.
15. Allworth AE, Albertini DF. Meiotic maturation in cultured bovine oo-

cytes is accompanied by remodeling of the cumulus cell cytoskeleton. Dev Biol 1993; 158:101–112.
16. Šutovský P, Fléchon JE, Fléchon B, Motlik J, Peynot N, Chesné P, Heyman Y. Dynamic changes of gap junction and cytoskeleton during in vitro culture of cattle oocyte cumulus complexes. Biol Reprod 1993; 49:1277–1287.
17. Makabe S, Naguro T, Motta PM. A new approach to the study of ovarian follicles by scanning electron microscopy and ODO maceration. Arch Histol Cytol 1992; 55:182–190.
18. Kim NH, Day BN, Lee HT, Chung KS. Microfilament assembly and cortical granule distribution during maturation, parthenogenetic activation and fertilisation in the porcine oocyte. Zygote 1996; 4:145–149.
19. Koehler JK, Clark JM, Smith D. Freeze-fracture observations on mammalian oocyte. Am J Anat 1985; 174:317–329.
20. Fukudome H, Tanaka K. A method for observing intracellular structures of free cells by scanning electron microscopy. J Microsc 1986; 141:171–178.
21. Suzuki H, Azuma T, Koyama H, Yang X. Development of cellular polarity of hamster embryos during compaction. Biol Reprod 1999; 61:521–526.
22. Laurincík J, Pivko J, Kroslak P. Cumulus oophorus expansion of bovine oocytes cultured in vitro: a SEM and TEM study. Reprod Domest Anim 1992; 27:217–228.
23. von Weymarn N, Guggenheim R, Müller H. Surface characteristics of oocytes from juvenile mice as observed in the scanning electron microscope. Anat Embryol (Berl) 1980; 161:19–27.
24. Nogués PM, Ponsà M, Vidal F, Egozcue J. Effects of aging on the zona pellucida surface of mouse oocytes. J In Vitro Fertil Embryo Transfer 1988; 5:225–229.
25. Phillips DM, Shalgi R. Surface architecture of the mouse and hamster zona pellucida and oocyte. J Ultrastruct Res 1980; 72:1–12.
26. Familiari G, Nottola SA, Micara G, Aragona C, Motta PM. Human in vitro fertilization: the fine three-dimensional architecture of the zona pellucida. In: Motta PM (ed.), Developments in Ultrastructure of Reproduction. New York: Alan R. Liss; 1989: 335–344.
27. Familiari G, Nottola SA, Macchirelli G, Micara G, Aragona C, Motta PM. Human zona pellucida during in vitro fertilization: an ultrastructural study using saponin, ruthenium red, and osmium-thiocarbohydrazide. Mol Reprod Dev 1992; 32:51–61.
28. Motta PM, Nottola SA, Micara G, Familiari G. Ultrastructure of human unfertilized oocytes and polyspermic embryos in an IVF-ET program. In: Jones HWJ, Scheader C (eds.), In Vitro Fertilization and Other Assisted Reproduction. New York: New York Academy of Sciences; 1988: 367–383.
29. Jackowski S, Dumont JN. Surface alterations of the mouse zona pellucida and ovum following in vivo fertilization: correlation with the cell cycle. Biol Reprod 1979; 20:150–161.
30. Calafell JM, Nogués C, Ponsà M, Santaló J, Egozcu J. Zona pellucida surface of immature and in vitro matured mouse oocytes: analysis by scanning electron microscopy. J Assist Reprod Genet 1992; 9:365–372.
31. Wassarman PM. Zona pellucida glycoproteins. Annu Rev Biochem 1988; 57:415–442.
32. Duby RT, Hill JL, O'Callaghan D, Overstrom EW, Boland MP. Changes induced in the bovine zona pellucida by ovine and bovine oviducts. Theriogenology 1997; 47:332 (abstract).
33. Yanagimachi R. Mammalian fertilization. In: Knobil E, Neil J (eds.), The Physiology of Reproduction. New York: Raven Press; 1988: 135–185.
34. Anderson E, Albertini DF. Gap junctions between the oocyte and companion follicle cells in the mammalian ovary. J Cell Biol 1976; 71: 680–686.
35. Gilula NB, Epstein ML, Beers WH. Cell-to-cell communication and ovulation. A study of the cumulus-oocyte complex. J Cell Biol 1978; 78:58–75.
36. Hyttel P. Bovine cumulus-oocyte disconnection in vitro. Anat Embryol 1987; 176:41–44.
37. Kruip TAM, Cran DG, van Beneden TH, Dieleman SJ. Structural changes in bovine oocytes during final maturation in vivo. Gamete Res 1983; 8:29–47.
38. Moor RM, Smith MW, Dawson RM. Measurement of intercellular coupling between oocytes and cumulus cells using intracellular markers. Exp Cell Res 1980; 126:15–29.
39. Zamboni L. Fine morphology of the follicle wall and follicle cell-oocyte association. Biol Reprod 1974; 10:125–149.
40. Cran DG. Qualitative and quantitative structural changes during pig oocyte maturation. J Reprod Fertil 1985; 74:237–245.
41. Brackett BG, Younis AI, Fayer-Hosken RA. Enhanced viability after in vitro fertilization of bovine oocytes matured in vitro with high concentrations of luteinizing hormones. Fertil Steril 1989; 52:319–324.
42. Saeki K, Hoshi M, Leibfried-Rutledge ML, First NL. In vitro fertilization and development of bovine oocytes matured in serum-free medium. Biol Reprod 1991; 44:256–260.
43. Younis AL, Brackett BG, Fayer-Hosken RA. Influence of serum and hormones on bovine oocyte maturation and fertilization in vitro. Gamete Res 1989; 23:189–201.
44. Salustri A, Camaioni A, Giacome MD, Fulop C, Hascall VC. Hyaluron and proteoglycans in ovarian follicles. Hum Reprod Update 1999; 5:293–301.